

Lyapunov Instability of Dense Lennard-Jones Fluids

H. A. Posch
Institute for Experimental Physics, University of Vienna
Boltzmanngasse 5, A-1090 Vienna, Austria

and

W. G. Hoover
Department of Applied Science, University of California
at Davis--Livermore and Lawrence Livermore National Laboratory
University of California, Livermore, CA 94550

This paper was prepared for submittal to
Physical Review A



October 1987

Lawrence
Livermore
National
Laboratory

This is a preprint of a paper intended for publication in a journal or proceedings. Since changes may be made before publication, this preprint is made available with the understanding that it will not be cited or reproduced without the permission of the author.

CIRCULATION COPY
SUBJECT TO RECALL
IN TWO WEEKS

DISCLAIMER

This document was prepared as an account of work sponsored by an agency of the United States Government. Neither the United States Government nor the University of California nor any of their employees, makes any warranty, express or implied, or assumes any legal liability or responsibility for the accuracy, completeness, or usefulness of any information, apparatus, product, or process disclosed, or represents that its use would not infringe privately owned rights. Reference herein to any specific commercial products, process, or service by trade name, trademark, manufacturer, or otherwise, does not necessarily constitute or imply its endorsement, recommendation, or favoring by the United States Government or the University of California. The views and opinions of authors expressed herein do not necessarily state or reflect those of the United States Government or the University of California, and shall not be used for advertising or product endorsement purposes.

Lyapunov Instability of Dense Lennard-Jones Fluids

by

H. A. Posch

**Institute for Experimental Physics, University of Vienna,
Boltzmanngasse 5, A-1090 Vienna, Austria,**

and

W. G. Hoover

**Department of Applied Science, University of California
at Davis - Livermore and Lawrence Livermore National Laboratory,
University of California, California 94550, USA.**

To be published in Physical Review A

Number of pages: 26

Number of tables: 3

Number of figures: 5

PACS numbers: 05.45.+b
 05.70.Ln
 05.20.-y
 46.10.+z
 47.50.+d
 65.50.+m

Abstract *

We present calculations of the full spectra of Lyapunov exponents for 8- and 32-particle systems in three dimensions with periodic boundary conditions and interacting with the repulsive part of a Lennard-Jones potential. A new algorithm is discussed which incorporates ideas from control theory and constraint nonequilibrium molecular dynamics. Equilibrium and nonequilibrium steady states are examined. The latter are generated by the application of an external field \underline{F}_e through which an equal number of particles are accelerated in opposite directions, and by thermostating the system using Nosé-Hoover or Gauss mechanics. In equilibrium ($\underline{F}_e=0$) the Lyapunov spectra are symmetrical and may be understood in terms of a simple Debye model for vibrational modes in solids. For nonequilibrium steady states ($\underline{F}_e \neq 0$) the Lyapunov spectra are not symmetrical and indicate a collapse of the phase-space density onto an attracting fractal subspace with an associated loss in dimensionality proportional to the square of the applied field. Because of this attractor's vanishing volume in phase-space and the instability of the corresponding repeller it is not possible to observe trajectories violating the second law of thermodynamics in spite of the time reversal invariance of the equations of motion. Thus, Nosé-Hoover mechanics, of which Gauss' isokinetic mechanics is a special case, resolves the reversibility paradox first stated by Loschmidt in 1876 for nonequilibrium steady state systems.

*This work was performed under the auspices of the U.S. Department of Energy by Lawrence Livermore National Laboratory under contract No. W-7405-Eng-48.

1. Introduction

In recent years many chaotic continuous-time systems have been studied, both experimentally and by computer simulation. A useful way to characterize their stochastic properties is the spectrum of Lyapunov characteristic exponents $\{\lambda_i\}$ describing the mean exponential rates of divergence and convergence of neighboring trajectories in phase space [1-6]. For chaotic systems the largest Lyapunov exponent is positive, whereas regular motion exhibiting fixed points, limit cycles or KAM-tori leads to Lyapunov exponents ≤ 0 . Furthermore, the sum of all positive Lyapunov exponents is the Kolmogorov entropy [4,6].

For any flow in M-dimensional phase-space described by the set of first order differential equations,

$$\dot{\underline{\Gamma}} = \underline{G}(\underline{\Gamma}) \quad (1.1)$$

$$\underline{\Gamma} = \{x_i\}, \quad i = 1, 2, \dots, M \quad (1.2)$$

there are M Lyapunov exponents of which at least one must vanish [6]. In dissipative flows such as the famous Lorenz model of turbulence or the Navier-Stokes equations of continuum mechanics the phase-space volume is not conserved but shrinks, in the course of time, resulting in the appearance of a strange attractor. As a result the spectrum of Lyapunov exponents is not symmetrical around zero, and the sum of all exponents is negative. Two different connections between the Lyapunov spectrum and the fractal dimension of the strange attractor have been conjectured by Kaplan and Yorke [7,8] and Mori [9]. However, if the flow (1.1) is derived from an Hamiltonian at constant internal energy, the spectrum of Lyapunov exponents is symmetrical around zero,

$$\lambda_i = \lambda_{M-i+1} \quad (1.3)$$

and two of the exponents must vanish. Any further constant of the motion (such as one component of linear momentum) causes two of the remaining Lyapunov exponents to vanish.

In this paper we are concerned with the calculation of the full Lyapunov spectrum of a system of N particles interacting via a repulsive Lennard-Jones potential

$$\phi(r) = \begin{cases} 4\epsilon \left[\left(\frac{\sigma}{r} \right)^{12} - \left(\frac{\sigma}{r} \right)^6 \right] + \epsilon, & r < 2^{1/6} \sigma \\ 0, & r \geq 2^{1/6} \sigma \end{cases} \quad (1.4)$$

The total potential energy is assumed to be pairwise additive:

$$\Phi = \sum_{i < j} \phi(r_{ij}) \quad (1.5)$$

where r_{ij} is the distance between particles i and j . Both equilibrium and stationary nonequilibrium states are considered. Since the center of mass motion is conserved, there are $M = 6(N-1)$ Lyapunov exponents and $M(M+1)$ first order differential equations to be solved simultaneously (see section 3). To keep this number below a tolerable limit we treat the cases of $N=8$ and $N=32$ particles corresponding to 1,806 and 34,782 differential equations, respectively. We find that in the equilibrium liquid case the Lyapunov spectra have a very simple appearance and follow a power law in agreement with a previous model-calculation for a somewhat simplified interaction potential [10,11]. We defer the discussion of our results to sections 4 and 5.

The nonequilibrium situation is realized by introducing in the Hamiltonian a constant external field \underline{F}_0 through which half of the particles are accelerated towards opposite directions, respectively. For this "color" - conductivity problem to achieve steady state conditions a homogeneous Gauss thermostat is used [12-14]. In this method the equations of motion of all particles

are modified by the introduction of a constraint force designed to keep the kinetic energy K of the system equal to a constant value K_0 :

$$\dot{\underline{r}} = \begin{cases} \dot{\underline{q}} = \underline{p}/m \\ \dot{\underline{p}} = \underline{F}(\underline{q}) - \zeta_G \underline{p} \end{cases} \quad (1.6)$$

Here, \underline{q} and \underline{p} are the positions and momenta of the particles, respectively,

$$\underline{F}(\underline{q}) = - \frac{\partial \Phi}{\partial \underline{q}} + c \underline{F}_e \quad (1.7)$$

is the total intrinsic force acting on a particle and \underline{F}_e is an external force, c being +1 for half of the particles and -1 for the other half. The constraint force term $-\zeta_G \underline{p}$ contains a thermostat variable ζ_G identical for all particles and determined at any instant of time from

$$\zeta_G = \frac{\frac{1}{m} \sum \underline{F}(\underline{q}) \cdot \underline{p}}{\frac{1}{m} \sum \underline{p} \cdot \underline{p}} \quad (1.8)$$

In this "isokinetic" simulation the phase-space dimension and consequently the number of Lyapunov exponents is the same as in Hamiltonian mechanics ($\zeta_G = 0$). Since the kinetic energy is a constant of the motion, again two of the exponents vanish in the equilibrium case ($\underline{F}_e = 0$) as compared to one in the nonequilibrium simulation ($\underline{F}_e \neq 0$). For the latter the sum of all Lyapunov exponents is found to be negative. The consequences of this important finding will be discussed in section 5.

An even more general modification of Hamiltonian mechanics has been recently invented by Nosé [15-17] making it possible to control independent thermodynamic variables during a simulation of a dynamical system through integral feedback both in equilibrium and nonequilibrium states [18-22]. In the formulation of Hoover [18,19,14] the equations of motion

generating isothermal flow assume the form

$$\dot{\Gamma} = \begin{cases} \dot{\underline{q}} = \underline{p}/m \\ \dot{\underline{p}} = \underline{F}(\underline{q}) - \zeta \underline{p} \\ \dot{\zeta} = \frac{1}{\tau^2} \left(\frac{K}{K_0} - 1 \right) \end{cases} \quad (1.9)$$

where $\underline{F}(\underline{q})$ is given by (1.7). Because of linear momentum conservation and the inclusion of the thermostat variable ζ as an independent variable, the phase space dimension and consequently the number of Lyapunov exponents is $6(N-1)+1$. $K = \sum \underline{p}^2/2m$ is the kinetic energy and $K_0 = 3NkT/2$ its long time averaged value. In thermostatted equilibrium ($\underline{F}_e=0$) the corresponding distribution function turns out to be canonical,

$$f_{\zeta} = \frac{\exp\{-H(\Gamma)/kT\}}{\int d\Gamma \exp\{-H(\Gamma)/kT\}} \quad (1.10)$$

where the internal energy of the total system (including the thermostat) is defined by

$$H(\Gamma) = K + \Phi + 3NkT\tau^2\zeta^2/2 \quad (1.11)$$

τ is an unspecified parameter related to the response time of the thermostat. In the limit of infinitely fast response ($\tau \rightarrow 0$) Nosé's isothermal dynamics becomes indistinguishable from Gaussian isokinetic flow (1.6).

It is important to notice that both the Gauss and Nosé equations of motion are invariant with respect to time reversal. In Nosé's original Hamiltonian the friction variable ζ arises as a momentum variable and consequently changes sign in the time-reversed motion as well as the particle momenta \underline{p} , whereas the coordinates \underline{q} and forces $\underline{F}(\underline{q})$ remain unchanged.

As a simple illustration of how Nosé-mechanics works the one-dimensional problem of a particle in a constant external field F_e will be treated in the following section. In section 3

various methods for calculating the complete spectrum of Lyapunov exponents for many body equilibrium and nonequilibrium systems are discussed. The results of our calculations are presented in section 4 and are further discussed in section 5.

2. One-dimensional "Nosé-Hoover" dynamics of a particle in a constant field.

As a simple illustration of Nosé-Hoover mechanics we consider the one-dimensional motion of a particle in a constant external field F_e . Since the long time averaged kinetic energy assumes the value $K_0 = kT/2$, where T is the temperature maintained by the Nosé thermostat, the equations of motion obtained from (1.8) are:

$$\begin{aligned}\dot{q} &= p/m \\ \dot{p} &= F_e - \zeta p \\ \dot{\zeta} &= \frac{1}{\tau^2} \left(\frac{p^2}{m k T} - 1 \right).\end{aligned}\tag{2.1}$$

The friction variable ζ becomes more negative whenever energy is to be fed into the system, and more positive when energy is to be extracted. A projection of possible trajectories onto the $(p\zeta)$ -plane is depicted in Fig.1 for a reduced thermostat response time $\tau(F_e/\sqrt{mkT}) = 1$. The flow equations (2.1) are time-reversible with p and ζ replaced by $-p$ and $-\zeta$ in the time-reversed motion. This corresponds to inversion through the origin in Fig.1. The motion in q direction becomes uniform for $t \rightarrow \infty$ and is associated with a Lyapunov exponent $\lambda_1 = 0$. The stable fixed point $(\sqrt{mkT}, F_e/\sqrt{mkT})$ in $(p\zeta)$ -space is an attractor characterized by Lyapunov exponents $\lambda_{2,3} = -F_e/2\sqrt{mkT}$, if the thermostat response time $\tau < \sqrt{8mkT}/F_e$. Time reversal transforms this attractor into an unstable fixed point $(-\sqrt{mkT}, -F_e/\sqrt{mkT})$ which is called a repellor and which is characterized by positive Lyapunov exponents. The flow in Fig.1 is reminiscent of a dollar sign, always leaving the vicinity of the repellor and heading for the attractor. This is true both in the original and the

time-reversed case.

This simple example serves to introduce the concept of a repeller as a set obtained from an attracting set by invoking a time reversal transformation. We shall use it in section 5 to discuss the irreversible behavior of steady-state nonequilibrium systems.

3. Computational methods.

Basically two algorithms for the calculation of the complete spectrum of Lyapunov exponents have been proposed [23,24,5,2,3]. In all these schemes - in addition to the reference trajectory (1.1) - M further trajectories are calculated, which are differentially separated from the reference trajectory and which obey the set of linearized equations of motion obtained by differentiating (1.1):

$$\frac{d}{dt} (\delta \underline{\Gamma})_{\ell} \equiv \dot{\underline{\delta}}_{\ell} = \underline{\underline{D}} \cdot \underline{\delta}_{\ell} ; \quad \ell = 1, 2, \dots, M. \quad (3.1)$$

Here, the coefficient matrix

$$\underline{\underline{D}}(\underline{\Gamma}) = \frac{\partial \underline{G}(\underline{\Gamma})}{\partial \underline{\Gamma}} \quad (3.2)$$

is an $M \times M$ matrix and couples the reference trajectory to the various differential offset vectors $\underline{\delta}_{\ell}$ in "tangent space". An arbitrarily oriented set of orthonormal vectors may be chosen as initial conditions for the M different vectors $\underline{\delta}_{\ell}$. However, as is well established for chaotic systems, these vectors do not stay orthogonal to each other for $t > 0$ but start rotating into the direction of maximum phase-space growth and eventually diverge. To avoid this problem a Gram-Schmidt reorthonormalization procedure may be repeatedly applied to the vector frame $\{\underline{\delta}_{\ell}\}$ after every few timesteps [24,5,2]. In this way we obtain that - after some transient time - $\underline{\delta}_1$ tends to point into the direction of phase space growing most rapidly proportional to $\exp \lambda_1 t$, that $\underline{\delta}_1, \underline{\delta}_2$ span a subspace whose area grows most rapidly proportional to $\exp(\lambda_1 + \lambda_2)t$, and so forth. Generally, $\underline{\delta}_1, \underline{\delta}_2, \dots, \underline{\delta}_{\ell}$ span a subspace with maximum volume growth proportional to $\exp(\lambda_1 + \lambda_2 + \dots + \lambda_{\ell})t$. From this sequence $\lambda_1, \lambda_2, \dots, \lambda_{\ell}$ may be

obtained. Most determinations of Lyapunov exponents have made use of this algorithm we shall refer to as "method A" [2,5,6].

As an alternative to the Gram-Schmidt reorthonormalization scheme a matrix orthogonalization technique has been proposed by Eckmann and coworkers [3] (method B).

We have recently introduced a third method [10,25] henceforth referred to as "method C" utilizing ideas from control theory and constraint dynamics [14]. This approach has been also suggested by Goldhirsch et.al.[26]. Instead of allowing the linearized trajectories (3.1) to evolve freely and calculating the Lyapunov exponents by periodically rescaling the differential offset vectors $\underline{\delta}_i$ in tangent space as in method A, these vectors may be constrained to stay normalized and orthogonal to each other at all times :

$$\underline{\delta}_i^t(t) \cdot \underline{\delta}_j(t) = \delta_{ij} \quad (3.3)$$

(δ_{ij} is Kronecker's symbol and t denotes the transpose). To achieve this, constraint "forces" must be introduced into the evolution equations (3.1):

$$\begin{aligned} \dot{\underline{\delta}}_1 &= \underline{D} \cdot \underline{\delta}_1 - \lambda_{11} \underline{\delta}_1 \\ \dot{\underline{\delta}}_2 &= \underline{D} \cdot \underline{\delta}_2 - \lambda_{21} \underline{\delta}_1 - \lambda_{22} \underline{\delta}_2 \\ &\vdots \\ \dot{\underline{\delta}}_M &= \underline{D} \cdot \underline{\delta}_M - \lambda_{M1} \underline{\delta}_1 - \lambda_{M2} \underline{\delta}_2 - \dots - \lambda_{MM} \underline{\delta}_M \end{aligned} \quad (3.4)$$

The magnitude of the constraint forces is governed by Lagrange multipliers λ_{ij} which may be calculated from the requirements (3.3). For example, differentiating (3.3) for $i=j$, we find:

$$\underline{\delta}_i^t \cdot \dot{\underline{\delta}}_i = 0$$

Insertion of $\dot{\underline{\delta}}_i$ from (3.4) gives for the main diagonal elements:

$$\lambda_{ii} = \underline{\delta}_i^t \cdot \underline{D} \cdot \underline{\delta}_i, \quad i = 1, 2, \dots, M. \quad (3.5)$$

Similarly, we find for $i \neq j$

$$\underline{\dot{\underline{\underline{d}}}}_i^t \cdot \underline{\dot{\underline{\underline{d}}}}_j + \underline{\dot{\underline{\underline{d}}}}_j^t \cdot \underline{\dot{\underline{\underline{d}}}}_i = 0$$

and

$$\lambda_{ij} = \underline{\dot{\underline{\underline{d}}}}_j^t \cdot \underline{\underline{D}} \cdot \underline{\dot{\underline{\underline{d}}}}_i + \underline{\dot{\underline{\underline{d}}}}_i^t \cdot \underline{\underline{D}} \cdot \underline{\dot{\underline{\underline{d}}}}_j. \quad (3.6)$$

The time evolution of $\underline{\underline{d}}_1, \underline{\underline{d}}_2, \dots, \underline{\underline{d}}_M$ is a rotation in tangent space where an arbitrarily oriented set of orthonormal vectors may serve as initial condition for the set $\{\underline{\underline{d}}_e(0)\}$. The Lyapunov exponents are given by the time averaged diagonal elements of the Lagrange multipliers :

$$\lambda_i = \frac{1}{t_{\max}} \int_0^{t_{\max}} \lambda_{ii} dt \quad (3.7)$$

The theoretical merits of method C are twofold: Firstly, the Lyapunov exponents are evaluated directly from the evolution equations (3.4) with their symmetry properties with respect to time reversal explicitly displayed. Secondly and more important, the angular velocities ω_e of the rotating set of orthonormal vectors $\{\underline{\underline{d}}_e\}$ are related to the frequencies of collective excitations or phonon frequencies of the system. This will be shown in more detail in a forthcoming publication. In this connection it is useful to recognize that the dynamical behavior of the orthonormal set $\{\underline{\underline{d}}_e\}$ is local in phase-space. By this we mean that the Lagrange multipliers λ_{ij} and consequently the angular velocities ω_e depend only on the instantaneous phase-point $\underline{\Gamma}(t)$. They may be generated by starting at $\underline{\Gamma}(t)$ and integrating the reference trajectory (1.1) backward in time for a time interval Δt . At $\underline{\Gamma}(t-\Delta t)$ an arbitrarily oriented set of orthonormal unit vectors $\{\underline{\underline{d}}_e(t-\Delta t)\}$ may be used as initial condition for a subsequent integration forward in time of both (1.1) and (3.4) to find the current $\{\underline{\underline{d}}_e(t)\}$, λ_{ij} and ω_e at $\underline{\Gamma}(t)$. For large enough time intervals Δt the result will be independent

of the initial conditions for $\{\underline{q}_\ell\}$ at $t-\Delta t$. The local frequencies ω_ℓ may become useful for semiclassical path-integral methods introduced recently [27].

There are, however, some problems in a practical implementation of method C. The extensive vector-matrix operations in (3.5) and (3.6) necessary at each timestep decrease the calculation speed on a VAX-750 computer by a factor of 4 as compared to method A for the calculation of the full Lyapunov spectrum of an eight particle system in 3 dimensions ($M=42$). Another minor problem arises from the restricted computational accuracy. Minor deviations are magnified in the course of time resulting in a noticeable violation of the condition (3.3) after a certain number of timesteps. However, this can be easily remedied by a periodic application of the Gram-Schmidt reorthonormalization scheme with negligible expense in computer time.

In a practical realization of method C a convenient way of performing the time averages over the Lyapunov exponents (3.7) or of any other dynamical quantities such as the potential energy Φ is to add these quantities to the list of variables $\{\dot{\underline{r}}, \dot{\underline{z}}, \dots, \dot{\underline{z}}_M\}$ integrated by the integration method in use. For all our simulation results reported in the following section a fourth order Runge-Kutta integration with a reduced timestep of 0.001 was employed. Reduced units with m, σ and ϵ acting as units of mass, length and energy together with periodic boundary conditions are used. The Lyapunov spectra obtained by methods A and C for the 8-particle systems agreed to better than 5% if in both runs the trajectories were followed for 10^5 timesteps. It is interesting to note that in very stiff systems the off-diagonal Lagrange multipliers λ_{M_i} associated with the most negative Lyapunov exponent λ_M may become extremely large making it difficult for the algorithm to keep $\dot{\underline{z}}_M$ normalized and

orthogonal to all the other vectors $\underline{\phi}_1, \dots, \underline{\phi}_{M-1}$. If this happens Gram-Schmidt reorthonormalization must be used every few time steps to prevent the solution for λ_M to become unstable. For the 32-body fluids also reported in the following section only method A has been used.

4. Lyapunov spectra of 8- and 32-body fluids

Fig.2 shows Lyapunov spectra for three thermodynamic states of an equilibrium (isoenergetic) 8-body system obeying Hamiltonian equations of motion and periodic boundary conditions. All data are in reduced units. Only positive exponents are calculated and indicated by the symbols in this figure. The negative exponents can be easily obtained from the symmetry condition (1.3), where $M=42$. The exponents are arranged such that the index $n=(M/2)-i$, $i=1,2,\dots,M/2$, denotes the number of positive Lyapunov exponents less or equal to a given exponent, $\lambda(n)$. The spectra have a very simple appearance and do not exhibit any fine structure. They can be approximated well by a power law,

$$\lambda(n) = \alpha n^\beta \quad (4.1)$$

as shown by the smooth curves in Fig.2, which are extended also to the full range of negative Lyapunov exponents. The fit parameters α and β are collected in Table 1 together with relevant thermodynamic information on the states considered.

A very similar result has been found by us already for a simpler, but also purely repulsive pair potential [10,11]. Table 1 shows that the exponent β is close to $1/3$ in all cases, which is precisely the value derived from a Debye model for the distribution of vibrational frequencies in a solid. In such a model the number of modes dn between frequencies ν and $\nu+d\nu$ is proportional to ν^2 . Integrating this relation one finds $\lambda(n) \propto n^{1/3}$, which is of the form (4.1) with $\beta_{\text{Debye}} = 1/3$. As may be verified from Table 1, the maximum Lyapunov exponent λ_{max} is also close in value to the Debye frequency ν_D . The latter may be

estimated from the second derivative of the pair potential, $\phi''(R)$, calculated at the particle separation R for which $\phi(R) = kT$:

$$2\pi\nu_D = [\phi''(R)/m]^{1/2} \quad (4.2)$$

In figures 3 to 5 analogous spectra are shown for thermostatted isokinetic 8- and 32-body systems, where Gauss' equations of motion (1.6) have been applied. Let us discuss the case of field-free equilibrium first ($F_e = 0$ in fig.3 and 4). The power law (4.1) provides a good fit of the numerical Lyapunov spectra. The fit parameters and further relevant information for these systems is collected in tables 2 and 3, respectively. The exponent β is again in quite good agreement with the Debye result $1/3$, and the maximum Lyapunov exponent seems to agree satisfactorily with the estimation of ν_D based on (4.2). At first the rather close agreement of the Lyapunov spectra with predictions derived from a simple Debye model is surprising. In hindsight it appears plausible in view of the fact that the coefficient matrix (3.2) is formally similar to the expansion coefficients of the potential energy Φ in powers of atomic lattice site displacements used in the theory of lattice dynamics of harmonic solids [28]. However, a close inspection of figure 3 reveals systematic deviations of the numerically obtained points from the fit particularly at small values of λ and n . These deviations also persist whether method A or method C is used for the simulation of the spectra. It remains to be seen whether the inclusion of an attractive part to the pair potential has a noticeable influence on the shape of the Lyapunov spectra.

Nonequilibrium steady state results are shown in Figs.3 and 5. As expected, the application of an external field, $F_e \neq 0$, destroys the symmetry of the Lyapunov spectra. They are not shifted uniformly to more negative values of λ , but the positive branch

of the spectra decreases more strongly than the negative one. In tables 2 and 3 we also list the sum over all Lyapunov exponents which is equal to the phase-space "compressibility" averaged over the nonequilibrium ensemble:

$$\langle \mathcal{L} \rangle = \int d\Gamma f(\Gamma, t) \frac{\partial}{\partial \Gamma} \cdot \dot{\Gamma}(\Gamma, t) = \sum_{i=1}^M \lambda_i \quad (4.3)$$

Here, $f(\Gamma, t)$ is the distribution function obeying the general Liouville equation [27,22]

$$\frac{\partial f}{\partial t} + \frac{\partial}{\partial \Gamma} \cdot (f \dot{\Gamma}) = 0 \quad (4.4)$$

The tables 2 and 3 also contain the Kolmogorov entropy h_K , which according to Pesin is the sum over all positive Lyapunov exponents [28,6]:

$$h_K = \sum_{\lambda > 0} \lambda \quad (4.5)$$

h_K is the mean rate at which information about the system is lost in the course of time.

With the external field \underline{F}_e applied, the system experiences also a dissipative flux in the direction of the field, the color current, defined by

$$\underline{J} = \sum c_p / m \quad (4.6)$$

where $c=+1$ is the color introduced in (1.7). We have measured this quantity from which a steady-state color conductivity may be derived according to

$$\langle \underline{J} \rangle = V \alpha \underline{F}_e \quad (4.7)$$

α is also collected in the tables. The error bars for α are estimated from the numerical noise for the components of $\langle \underline{J} \rangle$ perpendicular to \underline{F}_e which theoretically should be zero.

5. Irreversibility in nonequilibrium steady-state systems

The internal energy of the system is defined by

$$H(\underline{\Gamma}) = \Phi + \sum \frac{p^2}{2m} . \quad (5.1)$$

Its rate of change is given by

$$\dot{H}(\underline{\Gamma}) = \dot{\underline{\Gamma}} \cdot \frac{\partial H}{\partial \underline{\Gamma}} = -2K_0 \zeta_G + \underline{J}(t) \cdot \underline{F}_e , \quad (5.2)$$

where (1.6,7) have been used, and \underline{J} is the dissipative flux defined in (4.6). The steady-state condition $\langle \dot{H} \rangle = 0$ therefore gives

$$\langle \zeta_G \rangle = \frac{1}{2K_0} \langle \underline{J} \rangle \cdot \underline{F}_e = \frac{V}{2K_0} \propto F_e^2 > 0 , \quad (5.3)$$

where in the second step we have used (4.7). The long time average of ζ_G acts as a positive friction coefficient removing the energy from the system which is continuously supplied by the external field.

For the phase-space compressibility we find:

$$\begin{aligned} \mathcal{L} &= \frac{\partial}{\partial \underline{\Gamma}} \cdot \dot{\underline{\Gamma}} = \sum \left(\frac{\partial}{\partial \underline{q}} \cdot \dot{\underline{q}} + \frac{\partial}{\partial \underline{p}} \cdot \dot{\underline{p}} \right) = \\ &= -3(N-1)\zeta_G - \frac{1}{2K_0} \sum \left(\underline{p} \cdot \frac{\partial \Phi}{\partial \underline{q}} \right) - \frac{1}{2K_0} \underline{J} \cdot \underline{F}_e , \end{aligned} \quad (5.4)$$

where $3(N-1)$ gives the dimension of momentum space. Upon averaging the second term in (5.4) vanishes and we find:

$$\langle \mathcal{L} \rangle = -3(N-1)\langle \zeta_G \rangle - \frac{1}{2K_0} \langle \underline{J} \rangle \cdot \underline{F}_e . \quad (5.5)$$

Combining this equation with (5.3) yields

$$\langle \mathcal{L} \rangle = - [3(N-1) + 1] \frac{V}{2K_0} \propto F_e^2 . \quad (5.6)$$

Since $\langle \Lambda \rangle$ in (4.3) is equal to the sum of all Lyapunov exponents, (5.6) provides a convenient test of the numerical consistency of the data. We find very good agreement of $\langle \Lambda \rangle$, calculated from (5.6) with the parameters taken from tables 2 and 3, respectively, with $\sum \lambda$ for not too large fields $F_e \leq 2$.

For nonvanishing external fields the time averaged sum of Lyapunov exponents, $\sum \lambda = \langle \Lambda \rangle$, is always negative and varies according to (5.6) with the square of the applied field. This result has extremely interesting consequences and provides an understanding of the irreversible behavior of nonequilibrium steady-state systems in spite of the time reversal invariance of the equations of motion [29,30]. It means that an arbitrary hypervolume in phase-space centered on a trajectory shrinks in the course of time and develops into a very complicated fractal like object. That systems in nonequilibrium steady states develop into "strange attractors" has been first observed in simulations of a periodic two-dimensional classical Lorentz gas driven by an external field [31] and of a single-body, one-dimensional Frenkel-Kontorova model for isothermal electronic conduction [32]. The self-similar, sheet-like structure of these fractal attractors is clearly visible for the problems mentioned above involving a phase-space of only three dimensions. For the high-dimensional phase-spaces treated in this paper it is obviously not possible to generate similar plots. We proceed by evaluating the dimensionality of the strange attractors.

The Lyapunov dimension d_L may be estimated according to Kaplan and Yorke [7,8] from

$$d_L = j + \frac{\sum_{i=1}^j \lambda_i}{|\lambda_{j+1}|}, \quad (5.7)$$

where the integer j is determined from the conditions

$$\sum_{i=1}^j \lambda_i \geq 0, \quad \sum_{i=1}^{j+1} \lambda_i < 0. \quad (5.8)$$

The results for d_L are also listed in tables 2 and 3. It has been argued that the dimensionality loss of the phase-space attractors with respect to the equilibrium system (for which $d_L(0)=M$) is approximately given by

$$\Delta d_L \equiv d_L(F_e) - d_L(0) \approx \dot{S} / k \lambda_{\max} \quad (5.9)$$

where

$$S = -k \int d\Gamma f(\Gamma, t) \ln f(\Gamma, t) \quad (5.10)$$

is the information theory entropy. \dot{S} is the rate of irreversible entropy production and may be easily calculated [22]:

$$\begin{aligned} \dot{S}/k &= - \int d\Gamma \ln f \frac{\partial f}{\partial t} = - \int d\Gamma \ln f \left[-\frac{\partial}{\partial \Gamma} \cdot (f \dot{\Gamma}) \right] = \\ &= - \int d\Gamma \dot{\Gamma} \cdot \frac{\partial f}{\partial \Gamma} = \int d\Gamma f \frac{\partial}{\partial \Gamma} \cdot \dot{\Gamma} = \langle \mathcal{A} \rangle \end{aligned} \quad (5.11)$$

The first step follows from the normalization of f , the second from inserting the Liouville equation (4.4). The final steps follow from partial integration and the use of (5.4). We conclude that

$$\Delta d_L \approx \sum \lambda / \lambda_{\max} \quad (5.12)$$

This prediction is verified by our numerical results for not too large external fields, $F_e \leq 2$. Obviously the dimensionality loss is an extensive quantity and persists in the thermodynamic limit.

The fact that nonequilibrium systems quickly collapse onto a fractal subspace of the complete equilibrium phase-space with an associated loss in dimensionality is a general phenomenon. In addition to the problems mentioned above it has been observed also by Morriss in a study of planar two-bodey shear flow [33,34].

The consequences of this important result with respect to the second law of thermodynamics has been established very recently [29,30,32]: Only trajectories which on the average convert heat into work and which are characterized by a negative friction $\langle \zeta \rangle$ (or $\langle \zeta_G \rangle$) will violate the second law. In view of the time reversal invariance of the Nosé-Hoover or Gauss equations of motion (1.9) and (1.6), respectively, these trajectories must be precisely on the associated repellor and must be propagated backward in time. The repellor states are obtained from the strange attractor by the time reversal transformation $q \rightarrow q$, $p \rightarrow -p$, $\zeta \rightarrow -\zeta$ (or $\zeta_G \rightarrow -\zeta_G$) and consequently form again a fractal object with a dimensionality d_L less than the complete phase-space dimension M . Since time-reversal also means a sign change for the Lyapunov exponents the repellor states are characterized by a positive sum of Lyapunov exponents and a positive phase-space compressibility $\langle \Lambda \rangle$. It follows that the repellor is unstable: The slightest deviation will blow up very quickly and the trajectory will end up on the attractor again. One concludes (a) that an exact localization of the repellor is impossible because of its vanishing phase-space volume, and (b) that any approximate effort to localize and follow a time-reversed trajectory on the repellor is impossible because of its inherent instability. Thus, trajectories violating the second law do not occur in spite of the time reversal invariance of the equations of motion. Nosé-Hoover mechanics (1.9) - including Gauss' isokinetic equations (1.6) as a special case - therefore resolves the famous reversibility paradox first stated by Loschmidt in 1876 [35] and discussed further by Boltzmann [36], for the special case of nonequilibrium steady states.

Acknowledgements

We thank Dr. Brad Holian for many valuable discussions and Dr. Stronzo Bestiale for his continued interest in this work. Partial support was provided by a grant from the Austrian Fonds zur Förderung der wissenschaftlichen Forschung, projects P5455 and P5455A. We also acknowledge generous allocation of computer time by the Prozessrechenanlage Physik of the University of Vienna. The National Science Foundation again furnished generous travel support.

References

- [1] R.H.G.Helleman, "Self-generated chaotic behavior in nonlinear mechanics", in
Fundamental problems in Statistical Mechanics V,
E.G.D.Cohen, Editor, North Holland, Amsterdam 1980, p.165.
- [2] A.Wolf, J.B.Swift, H.L.Swinney and J.A.Vastano, "Determining Lyapunov exponents from a time series", Physica, 16D, 285(1985).
- [3] J.-P.Eckmann and D.Ruelle, "Ergodic theory of chaos and strange attractors", Rev.Mod.Phys., 57, 617(1985); addendum: Rev.Mod.Phys., 57, 1115(1985).
- [4] G.Benettin, L.Galgani and J.-M.Strelcyn, "Kolmogorov entropy and numerical experiments", Phys.Rev., A 14, 2338(1976).
- [5] I.Shimada and T.Nagashima, "A Numerical Approach to Ergodic Problem of Dissipative Dynamical Systems", Progr.Theor.Physics 61, 1605(1979).
- [6] A.J.Lichtenberg and M.A.Lieberman, Regular and Stochastic Motion, Springer, New York, 1983.
- [7] J.Kaplan and J.Yorke, "Chaotic behavior of multidimensional difference equations" in:
Functional Differential Equations and the
Approximation of Fixed Points, Lecture Notes in Mathematics 730, H.O.Peitgen and H.O.Walther, Editors, Springer, Berlin, 1978.
- [8] P.Frederikson, J.Kaplan, E.Yorke and J.Yorke, "The Lyapunov Dimension of Strange Attractors", J.Diff.Eqs., 49, 185(1983).

- [9] H.Mori, "Fractal Dimensions of Chaotic Flows of Autonomous Dissipative Systems", Progr.Theor.Phys., 63, 1044(1980).
- [10] W.G.Hoover, H.A.Posch and S.Bestiale, "Dense-Fluid Lyapunov Spectra via Nonequilibrium Molecular Dynamics", J.Chem.Phys., in press (1987).
- [11] W.G.Hoover and H.A.Posch, "Direct Measurement of Equilibrium and Nonequilibrium Lyapunov Spectra", Phys.Lett.A 123,227(1987).
- [12] D.J.Evans, W.G.Hoover, B.H.Failor, B.Moran, A.J.C.Ladd, "Nonequilibrium molecular dynamics via Gauss's principle of least constraint", Phys.Rev.A 28, 1016 (1983)
- [13] D.J.Evans and W.G.Hoover, "Flows far from equilibrium via molecular dynamics", Ann. Rev. Fluid Mech. 18, 243 (1986)
- [14] W.G.Hoover, Molecular Dynamics, Lecture Notes in Physics 258, (Springer Verlag, Berlin 1986).
- [15] S.Nosé, "A molecular dynamics method for simulation in the canonical ensemble", Mol.Phys., 52, 255 (1984).
- [16] S.Nosé, "A unified formulation of the constant- temperature molecular dynamics methods", J.Chem.Phys. 81, 511(1984)
- [17] S.Nosé, "An extension of the canonical ensemble molecular dynamics method", Molec.Phys.57, 187(1986).
- [18] W.G.Hoover, "Canonical dynamics: Equilibrium phase- space distributions", Phys.Rev. A 31, 1695(1985).
- [19] D.J.Evans and B.L.Holian, "The Nosé-Hoover thermostat", J.Chem.Phys. 83, 4069(1985).
- [20] H.A.Posch, W.G.Hoover and F.J.Vesely, "Canonical dynamics of the Nosé oscillator: stability, order and chaos", Phys.Rev. A 33, 4253(1986).
- [21] B.L.Holian and W.G.Hoover, "Numerical test of the Liouville equation", Phys.Rev. A34, 4229(1986).
- [22] B.L.Holian, "Entropy evolution as a guide for replacing the Liouville equation", Phys.Rev.A 34, 4238(1986).

- [23] G.Benettin, L.Galgani, A.Giorgilli and J.M.Strelcyn, "Tous les nombres de Liapounov sont effectivement calculables", C.R.Acad.Sci., Paris, 286A, 431(1978).
- [24] G.Benettin, L.Galgani, A.Giorgilli and J.M.Strelcyn, "Lyapunov Characteristic Exponents for Smooth Dynamical Systems and for Hamiltonian Systems: A Method for computing all of them", Meccanica 15, 9(1980).
- [25] W.G.Hoover and H.A.Posch, "Direct measurement of Lyapunov exponents", Phys.Lett.A 113, 82(1985).
- [26] I.Goldhirsch, P.-L.Sulem and S.A.Orszag, "Stability and Lyapunov stability of dynamical systems: a differential approach and a numerical method", Physica 27D, 311(1987).
- [27] R.P.Feynman and H.Kleinert, "Effective classical partition functions", Phys.Rev.A34, 5080(1986).
- [28] A.A.Maradudin, E.W.Montroll and G.H.Weiss, Theory of Lattice Dynamics in the Harmonic Approximation, Academic Press, New York, 1963.
- [29] B.L.Holian and D.J.Evans, "Classical response theory in the Heisenberg picture", J.Chem.Phys. 83, 3560 (1985).
- [30] Ja.B.Pesin, "Characteristic Lyapunov exponents and smooth ergodic theory", Uspehi Mat.Nauk 32:4,55(1977); English translation: Russian Math.Surveys 32:4,55(1977).
- [31] B.L.Holian, W.G.Hoover and H.A.Posch, "Resolution of Loschmidt's Paradox: The Origin of Irreversible Behavior in Reversible Atomistic Dynamics", Phys.Rev.Lett. 59,10(1987).
- [32] W.G.Hoover, "Reversible Mechanics and Time's Arrow", Phys.Rev.A,(1987),in press.
- [33] B.Moran, W.G.Hoover and S.Bestiale, "Diffusion in a Periodic Lorentz Gas", J.Stat.Phys. 48,709(1987).

- [34] W.G.Hoover, H.A.Posch, B.L.Holian, M.J.Gillan, M.Mareschal, C.Massobrio and S.Bestiale, "Dissipative irreversibility from Nosé's reversible mechanics", Molec.Simulations 1, (1987).
- [35] G.P.Morriss, "The information dimension of the nonequilibrium distribution function", Phys.Lett.A 122,236(1987).
- [36] G.P.Morriss, "The Lyapunov Dimension of Two-body Planar Couette Flow", in press.
- [37] J.Loschmidt, "Über den Zustand des Wärmegleichgewichtes eines Systems von Körpern mit Rücksicht auf die Schwerkraft I.", Sitzungsberichte d.k.Ak.Wiss. (Wiener Ber.), 73,128(1876).
- [38] L.Boltzmann, "Bemerkungen über einige Probleme der mechanischen Wärmetheorie II: Über die Beziehung eines allgemeinen mechanischen Satzes zum zweiten Hauptsatz der Wärmetheorie", Sitzungsberichte d.k.Ak.Wiss. (Wiener Ber.), part II, 75,67(1877); English translation: S.G.Brush, Kinetic Theory, Vol.2, Irreversible Processes,188,Pergamon,Oxford,1966

State	I	II	III
V	16.0	16.0	22.87
T	0.85	0.70	0.684
$\langle K \rangle$ *)	10.20	8.40	8.21
$\langle \Phi \rangle$	1.80	1.42	0.79
$\langle E \rangle$	12.00	9.82	9.00
t_{max}	150	100	100
α	1.33	1.22	1.02
β	0.32	0.32	0.31
γ_D	3.22	3.03	3.01
λ_{max}	3.52	3.30	2.70
h_K	54.2	50.1	40.4

Table 1: Parameters characterizing the isoenergetic 8-body system studied in Fig.2. All quantities are given in reduced units. V is the volume, T the temperature, K the kinetic energy, Φ the potential energy, E the total energy. t_{max} is the time for which the trajectory was followed after the decay of transients. α and β are obtained by fitting (4.1) to the positive Lyapunov exponents. γ_D is an estimate for the Debye frequency and λ_{max} is the maximum Lyapunov exponent. $h_K = \sum_{\lambda > 0} \lambda$ is the sum over all positive exponents.

*) The center of mass velocity is kept constant.

F_e	0.0	1.0	2.0	3.0
V	16.0	16.0	16.0	16.0
T	1.0	1.0	1.0	1.0
K_0 *)	12.0	12.0	12.0	12.0
$\langle \Phi \rangle$	2.21	2.20	2.22	1.99
$\langle E \rangle$	14.21	14.20	14.22	13.99
t_{max}	220	56	350	88
α	1.27	-	-	-
β	0.37	-	-	-
ν_D	3.40	-	-	-
λ_{max}	3.79	3.72	3.67	3.37
h_K	57.6	56.4	53.8	47.5
$\sum \lambda$	0	-1.3	-5.9	-14.3
d_L	42	41.64	40.51	38.3
κ	-	0.094+0.013	0.099+0.004	0.108+0.007

Table 2: Parameters for the isokinetic 8-body simulations for various external fields F_e . All quantities are given in reduced units. In addition to the symbols explained in table 1, d_L denotes the Lyapunov dimension, κ the conductivity and $\sum \lambda$ the sum over all Lyapunov exponents.

*) The center of mass velocity is kept constant.

F_e	0.0	1.0	2.0	3.0
V	64.0	64.0	64.0	64.0
T	1.0	1.0	1.0	1.0
K_0 *)	48.0	48.0	48.00	48.00
$\langle \bar{\Phi} \rangle$	8.33	8.87	8.99	7.62
$\langle E \rangle$	56.33	56.87	56.99	55.62
t_{max}	5.8	26.0	10.4	8.4
α	0.634	-	-	-
β	0.385	-	-	-
ν_D	3.40	-	-	-
λ_{max}	3.66	3.66	3.57	3.18
h_K	242	238	225	181
$\sum \lambda$	0	-6.8	-27.1	-85
d_L	186.0	184.2	178.9	163
α	-	0.108+0.005	0.109+0.005	0.136+0.008

Table 3: Parameters for the isokinetic 32-body simulations for various external fields F_e . All quantities are given in reduced units and are explained in tables 1 and 2.

*) The center of mass velocity is kept constant.

Figure captions

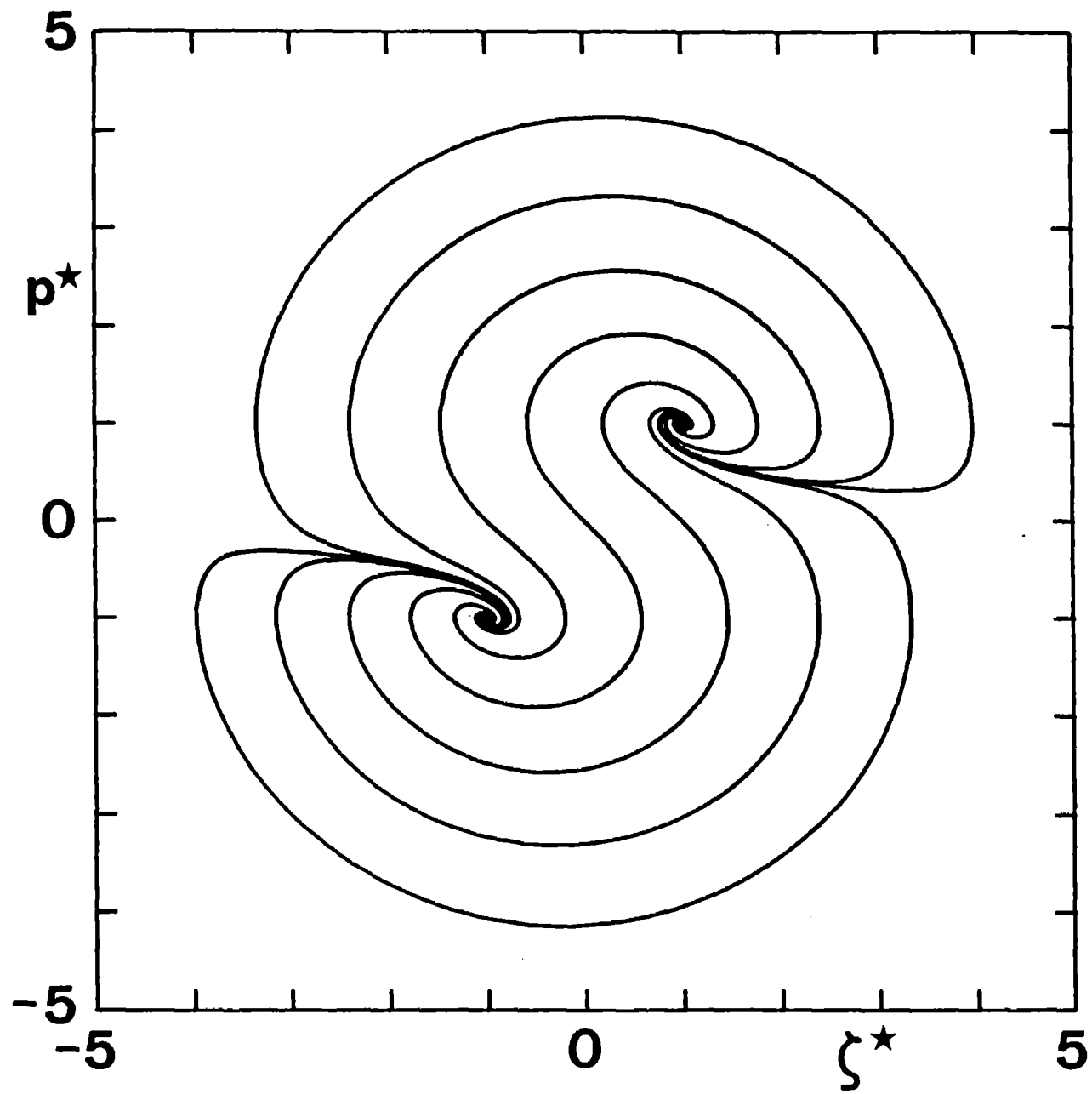
Fig.1 Projection of the flow (2.1) onto the $p\xi$ -plane for a reduced thermostat response time $\tau F_e / \sqrt{mkT} = 1$. $p^* = p / \sqrt{mkT}$, $\xi^* = \xi F_e / \sqrt{mkT}$.

Fig.2 Lyapunov spectra for an 8-body fluid in isoenergetic equilibrium for 3 thermodynamic states I, II and III specified in Table 1. Only positive exponents are calculated and indicated by the symbols. The smooth curves represent a fit of (4.1) to these data and are extended also to the full range of negative exponents. All quantities are in reduced units, with the potential parameters ε and σ of (1.4) and the mass m all set equal to unity

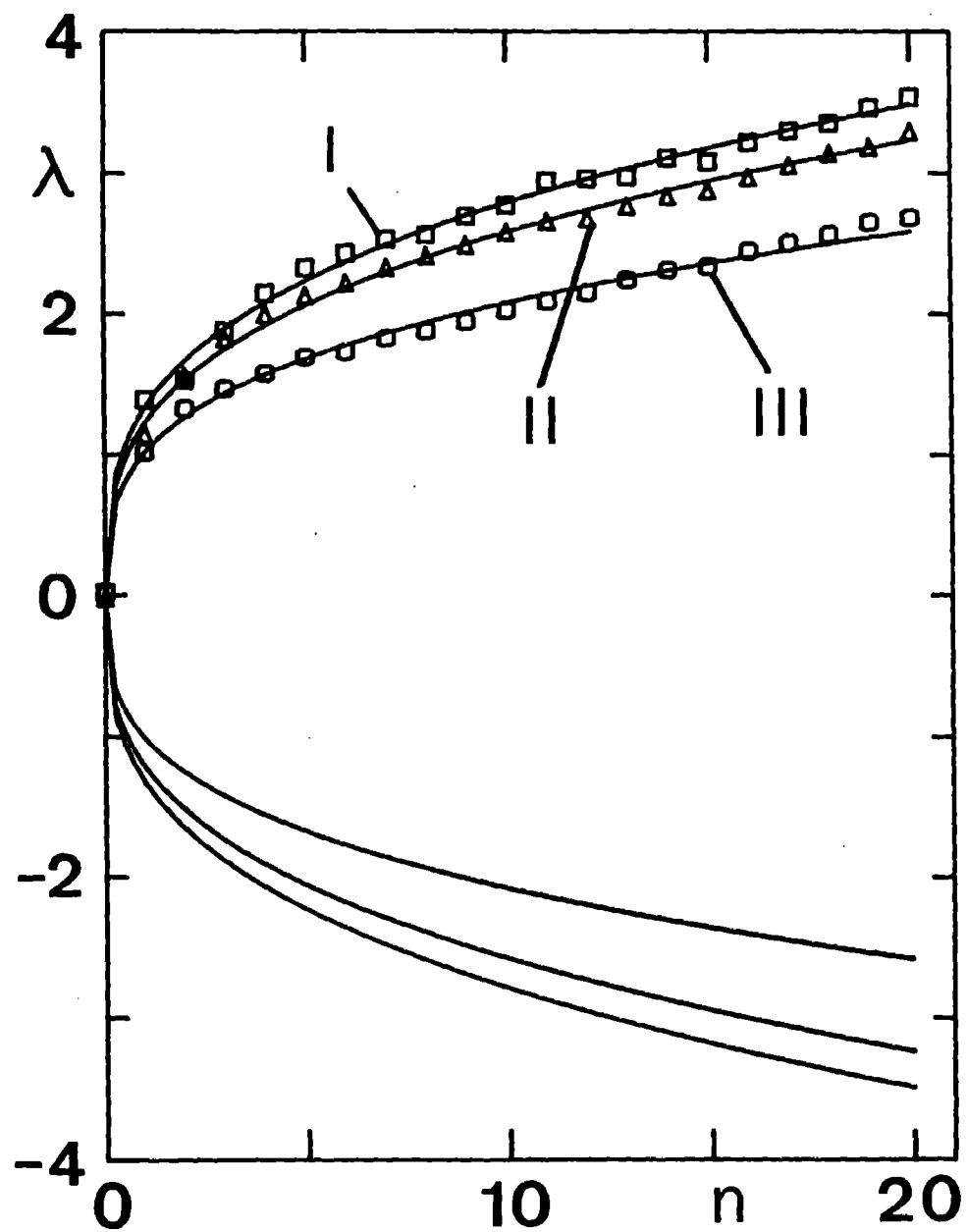
Fig.3 Full Lyapunov spectra for an isokinetic 8-body fluid for various reduced external fields F_e as indicated by the labels. The simulation results are shown as symbols, whereas the smooth line is a fit of (4.1) to the positive exponents for the equilibrium case ($F_e = 0$). Thermodynamic states and relevant parameters are listed in Table 2. All quantities are in reduced units as above.

Fig.4 Lyapunov spectrum for an isokinetic 32-body fluid at equilibrium ($\underline{F}_e=0$). Thermodynamic state parameters are listed in Table 2. Simulation results are indicated by the circles, whereas the smooth line is a fit of (4.1) to the positive exponents. All quantities are in reduced units as above.

Fig.5 Full Lyapunov spectra for an isokinetic 32-body fluid for various reduced external fields \underline{F}_e as indicated by the labels. The simulation results are shown as symbols. The smooth curve is a fit of (4.1) to the positive exponents for the equilibrium case ($\underline{F}_e=0$) depicted in Fig.4. Thermodynamic and related information is given in Table 3. All quantities are in reduced units as above.

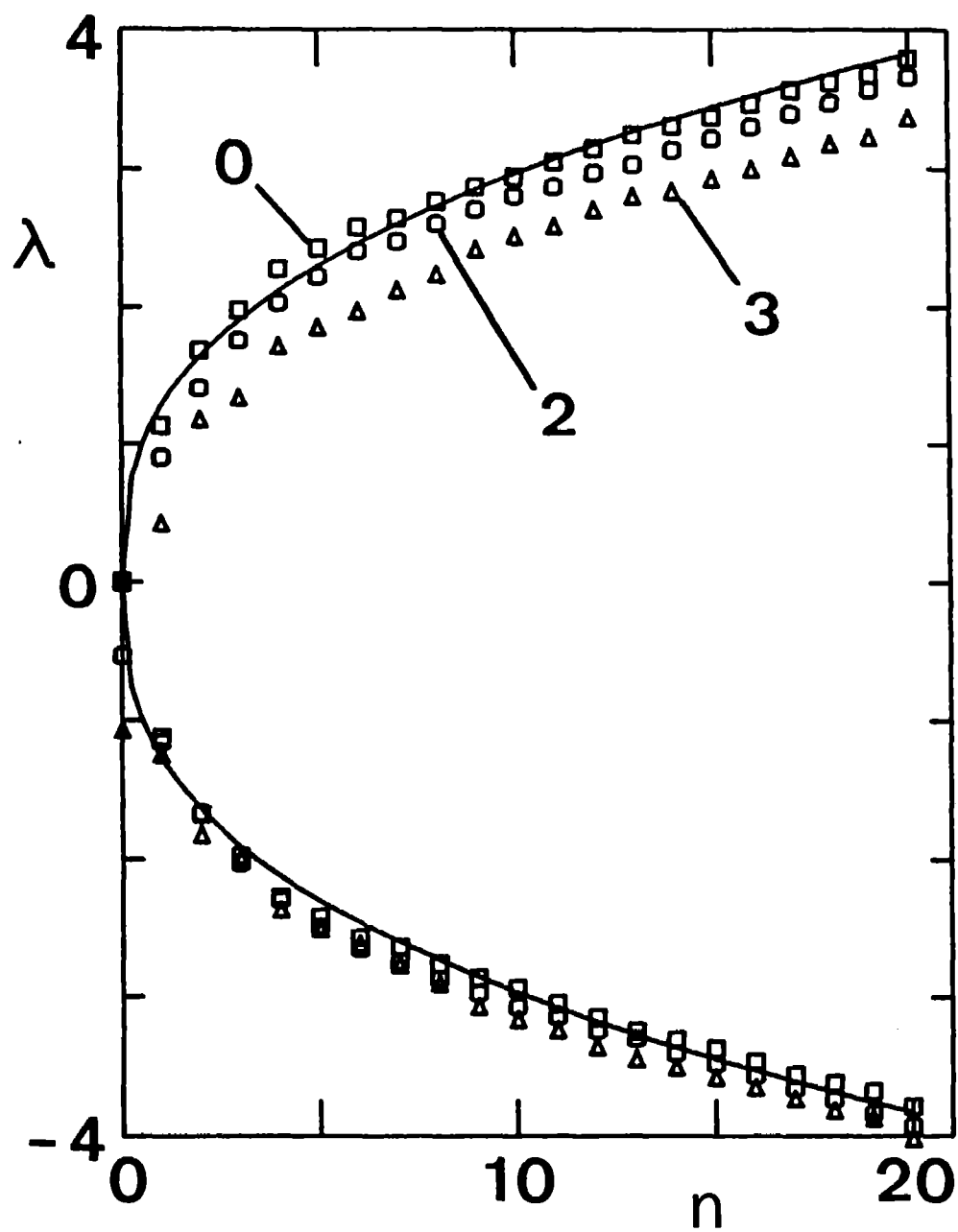


Posca - Hoover
Figure 1

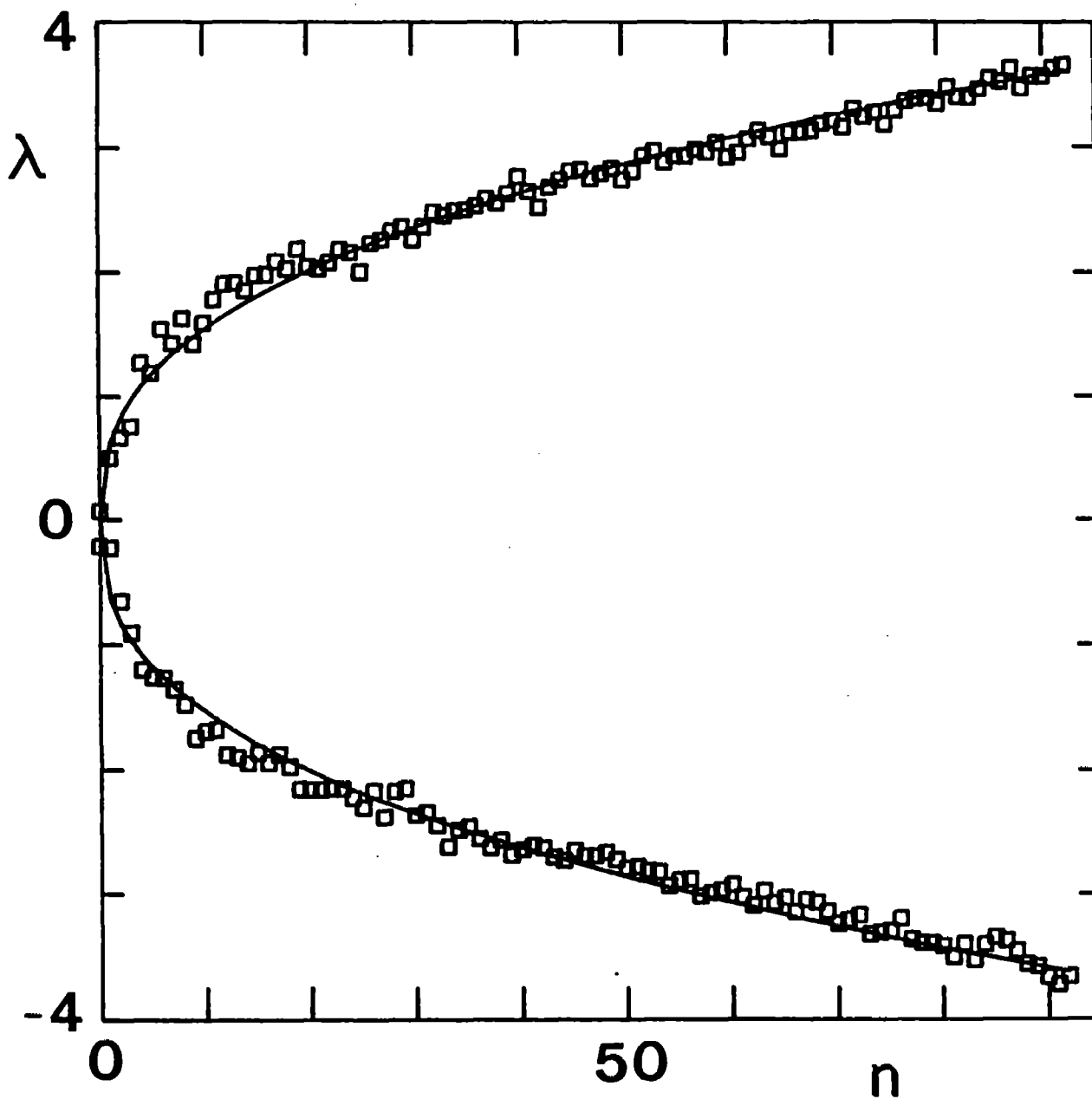


POSCH HOOVER

Figure 2

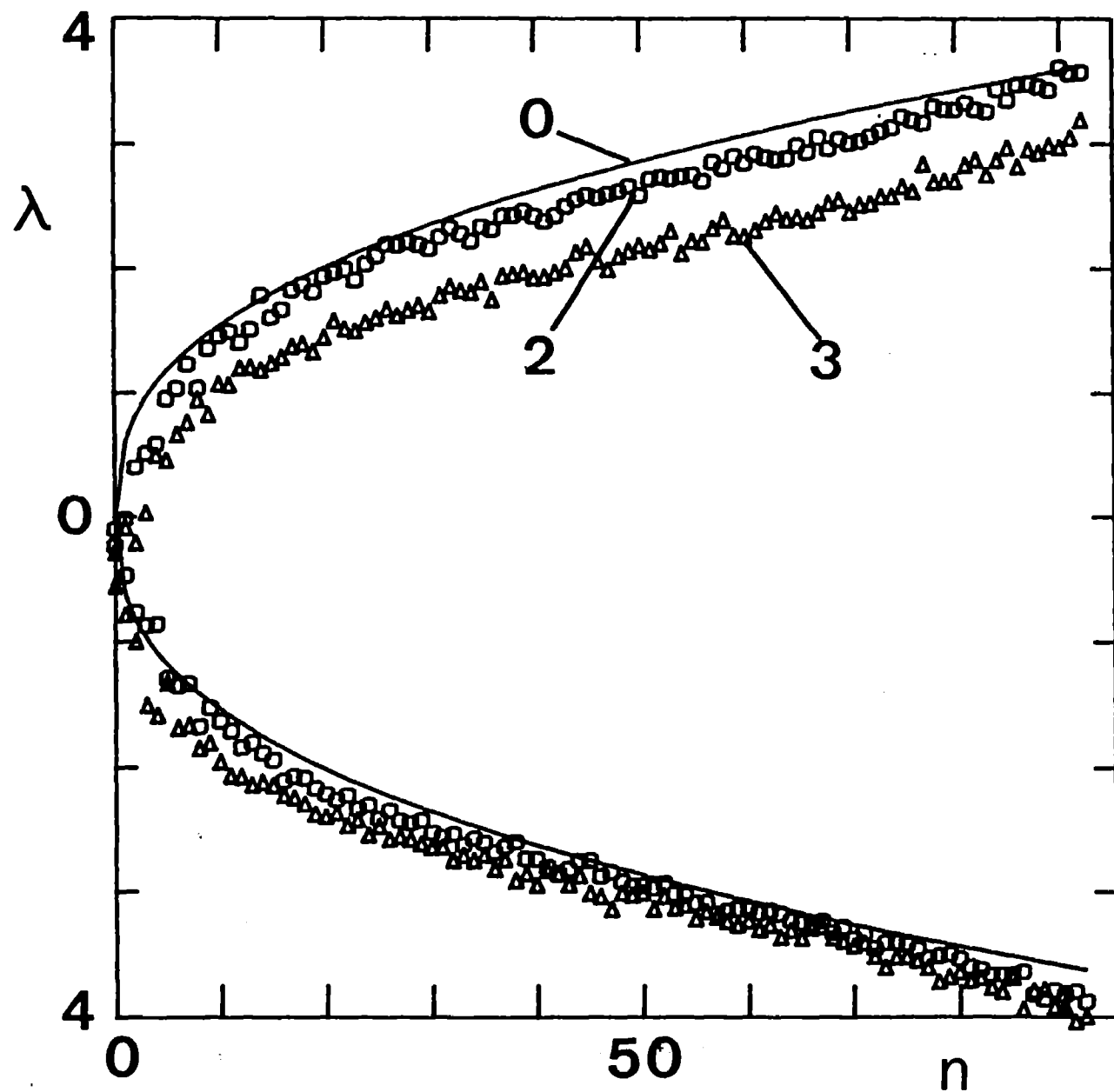


Posch-Hoover
Figure 3



Posch - Hoover

Figure 4.



POSCH HOOVER
FIGURE 5